M. A. Fayazbakhsh[1]
Laboratory for Alternative Energy Conversion,
School of Mechatronic Systems Engineering,
Simon Fraser University,
250-13450 102 Avenue,
Surrey, BC V3T 0A3, Canada
e-mail: mfayazba@sfu.ca

F. Bagheri
Laboratory for Alternative Energy Conversion,
School of Mechatronic Systems Engineering,
Simon Fraser University,
250-13450 102 Avenue,
Surrey, BC V3T 0A3, Canada

M. Bahrami
Laboratory for Alternative Energy Conversion,
School of Mechatronic Systems Engineering,
Simon Fraser University,
250-13450 102 Avenue,
Surrey, BC V3T 0A3, Canada

A Resistance–Capacitance Model for Real-Time Calculation of Cooling Load in HVAC-R Systems

Simulating the real-time thermal behavior of rooms subject to air conditioning (AC) and refrigeration is a key to cooling load calculations. A well-established resistance–capacitance (RC) model is employed that utilizes a representative network of electric resistors and capacitors to simulate the thermal behavior of such systems. A freezer room of a restaurant is studied during its operation, and temperature measurements are used for model validation. Parametric study is performed on different properties of the system. It is shown that a reduction of 20% in the walls thermal resistivity can increase the energy consumption rate by 15%. The effect of set points on the number of compressor starts/stops is also studied, and it is shown that narrow set points can result in a steady temperature pattern in exchange for a high number of compressor starts/stops per hour. The proposed technique provides an effective tool for facilitating the thermal modeling of air conditioned and refrigerated rooms. Using this approach, engineering calculations of cooling load can be performed with outstanding simplicity and accuracy.
[DOI: 10.1115/1.4030640]

1 Introduction

Heating, ventilation, air conditioning, and refrigeration (HVAC-R) contribute to a tremendous portion of energy consumption in a wide array of residential, industrial, and commercial applications worldwide. The energy consumption by HVAC-R systems is 50% of the total energy usage in buildings and 20% of the total national energy usage in European and American countries [1]. HVAC energy consumption can exceed 50% of the total energy usage of a building in tropical climates [2]. Furthermore, refrigeration systems also consume a substantial amount of energy. Supermarket refrigeration systems, as an example, can account for up to 80% of the total energy consumption in the supermarket [3].

Vehicle fuel consumption is also affected by AC in large scales. AC systems can reduce the fuel economy of today's midsized vehicles by more than 20% while increasing NO_x by approximately 80% and CO by 70% [4]. During regular commuting, the AC power consumption of midsized cars is estimated to be higher than 12% of the total vehicle power [5]. AC is a critical system for hybrid electric vehicles and electric vehicles, as it is the second most energy consuming system after the electric motor [6]. The energy required to provide cabin cooling for thermal comfort can reduce the range of plug-in electric vehicles (PEVs) from 35% to 50% depending on outside weather conditions [4].

Implementing opportunities to reduce energy consumption in HVAC-R systems can propagate by the above-mentioned scales to a large number of systems used in various applications. Predicting the cooling/heating load is a prerequisite to proper sizing, selection, and control of HVAC-R systems. As a result, any improvement in the calculation methods and the ability to predict the loads in real-time can result in significant reduction of total energy consumption and greenhouse gas emissions in large scales.

Ansari and Mokhtar [7] demonstrated that a great deal of mathematical complexities can be avoided in cooling load calculations without sacrificing accuracy. They suggested that hefty procedural details may be avoided with negligible loss of accuracy. Nevertheless, more complex approaches for thermal load estimation are also used in the literature, including neural networks [8,9], genetic algorithms [10,11], and fuzzy logic controllers [12]. These approaches cover a range of simplified to rigorous methods and have different levels of accuracy and engineering usability. Few of these methods are both accurate and easy-to-use.

American society of heating, refrigerating, and air conditioning (ASHRAE) has established extensive methodologies for calculation of heating and cooling loads [13]. The heat balance method (HBM) [14] is an example of such load calculation methods. It is a straight-forward and comprehensive method that involves calculating a wall-to-wall heat balance of a room through consideration of conductive, convective, and radiative heat transfer mechanisms. The method has been extensively used in residential [15] as well as nonresidential [16] applications. The essence of HBM is to calculate the overall heat flow across the walls of a room. For every wall, the heat flow encounters an outside convective resistance, a conduction across the wall, and an inside convective resistance. Some heat is also stored in the wall depending on its thermal inertia and temperature. After a balance of the incoming energy, the overall heat balance calculation is carried out for the room air.

Cooling/heating load calculations pertaining to HBM or other load calculation methods are greatly facilitated by RC modeling. RC modeling allows for better understanding of problem physics and makes it possible to easily evaluate modeling hypotheses and sensitivity to different parameters [17]. It is a well-recognized approach based on the analogy between thermal systems and electric circuits [18]. In this approach, the thermal system under consideration is represented by an equivalent electric circuit which is mathematically identical to the thermal system. RC modeling thus helps to visualize the HBM approach and solve the problem with better engineering insight. As an example, Bueno et al. [17] applied RC modeling to an urban canopy and evaluated their results against advanced simulation tools. They reported that the RC technique provides simplicity and computational efficiency, especially for studying the sensitivity of results to different parameters. In another work, Ogunsola et al. [19] deduced a time-series cooling load model from a simplified RC model to provide a

[1]Corresponding author.

Contributed by the Heat Transfer Division of ASME for publication in the Journal of Thermal Science and Engineering Applications. Manuscript received February 14, 2015; final manuscript received May 12, 2015; published online June 23, 2015. Assoc. Editor: Zahid Ayub.

thermal load estimation with manageable computational requirements. However, they used the RC approach for constructing the time-series formulation to predict future cooling loads, while the RC circuit can be directly used for simulating room temperature variations.

RC modeling is widely used in HVAC load calculations as well as other applications such as electronic cooling [20–24]. In HVAC applications, the thermal system is often divided into: (1) the room and (2) the envelope, i.e., the surrounding walls of the room. Each component can be modeled by a number of resistors and/or capacitors. For example, a 3R2C thermal model of a wall means that three resistors and two capacitors are used to represent it in its identical electric subcircuit. Since every wall or room is represented by an RC subcircuit, the complete model can become complicated with a large number of electrical components. Deng et al. [25] described a model reduction methodology used to obtain a simpler multiscale representation of the RC network. The original RC network of a building application consists of a large number of coupled linear differential equations. The proposed technique by Deng et al. [25] retains the physical intuition of the original model, but is a simpler RC network. However, their model reduction methodology was not compared with experimental data. RC modeling is also used for studies on specific parameters related to HVAC load calculations. Haldi and Robinson [26] developed a means for representing occupants' presence and behavior through RC modeling. They discussed a comprehensive representation of occupants and their activities in buildings. They used regression parameters to predict the probabilities of actions such as window and blind opening by occupants. Implementing these types of parameters in the HVAC design is highly facilitated by using the RC modeling approach.

Alongside residential AC, RC models are also used in mobile air conditioning and thermal energy storage applications. Mezrhab and Bouzidi [27] studied the thermal comfort inside a passenger car compartment according to climatic conditions and materials that compose the vehicle. They developed a numerical model based on the nodal method and solved the network using the finite difference method. Zhu et al. [28] utilized RC modeling for analyzing the application of phase change materials (PCM) for demand compensation of AC loads. They used a 3R2C model for the walls in series to a 4R2C model for the PCM layer.

An important issue regarding the usage of RC models in HVAC applications is the estimation of parameter values. Several thermal properties of the room and the envelope are often necessary which need to be acquired from comprehensive collection of data. In some cases, complex mathematical algorithms are incorporated to estimate these properties instead of directly acquiring them. Ogunsola et al. [19] used building construction data for envelope thermal properties, while genetic algorithm was used to estimate the internal thermal mass. Wang and Xu [10] obtained the RC parameters using a genetic algorithm and solved the integrated model numerically using Runge Kutta classical methods. Oldewurtel et al. [29] performed an investigation of how model predictive control (MPC) and weather predictions can increase the HVAC energy efficiency while maintaining occupant comfort. An RC network was constructed and employed for building climate control using MPC and weather forecasts. Maasoumy et al. [30] also used an MPC approach for energy efficient buildings. They used an RC representation of an office room to model the heat transfer paths. They proposed a parameter adaptive building model that facilitates the parameter tuning process in an online fashion in the MPC approach. Nevertheless, their approach adds to the complexity of the plain RC model. Platt et al. [31] focused on real-time HVAC zone model fitting and prediction techniques based on physical principles, as well as the use of genetic algorithms for optimization. They included supply air input in their model, but the thermal inertia of walls was ignored.

Table 1 summarizes the recent RC models used in HVAC applications. The RC subcircuit models used for the room and its envelope are also shown. Many of the mentioned methods depend on experimental measurements for acquiring the model parameters. Nevertheless, other approaches for "estimating" the RC parameters instead of "measuring" them are also named in Table 1.

In this study, the RC modeling approach is described as a method for comprehensive thermal simulation of HVAC-R systems. It can be readily applied to several applications such as residential AC, refrigeration, and vehicle thermal comfort analysis. As a case study, the approach is applied to the heat balancing of the entire space of a walk-in freezer room. Simulation of the refrigerated zone using an equivalent electric circuit facilitates the application of the HBM. It is shown that such an RC model can fully describe the thermal behavior of the refrigeration room. It helps the understanding and modeling of the thermal loads with reasonable accuracy. The model can be used as a simple engineering tool for correlating the variation of temperature and calculating thermal loads in real-time for a variety of HVAC-R applications. The RC modeling is also an excellent tool for retrofit analysis of existing HVAC systems. The advantages of the present RC modeling approach are summarized as follows:

- real-time simulation of HVAC-R thermal behavior
- enabling proactive control of HVAC-R systems
- direct measurement of thermal parameters instead of sophisticated mathematical estimations
- one RC circuit developed for the entire thermal system
- results validated with experimental data
- facilitating retrofit of existing HVAC-R systems through parametric studies

In the present work, the RC modeling technique is applied to a subzero freezer room. The RC circuit is further used for parametric studies on the effect of set points and thermal degradation of insulation materials. This study shows the capability of RC modeling for conducting such parametric studies, once the RC circuit is developed for a specific application. The rest of this paper is structured as follows: In Sec. 2, the fundamentals of RC modeling approach are described in its general form. In Sec. 3, the RC model is applied to a refrigeration application and the resulting electric circuit is demonstrated. Section 4 describes the model validation with experimental measurements as well as parametric studies on different parameters of the system. Finally, the conclusions from this study are summarized.

2 Model Development

A lumped thermal model of a room is developed based on the HBM and the RC modeling approach. The thermal model is first described in Sec. 2.1, followed by its RC equivalent in Sec. 2.2.

2.1 Thermal Model. Following ASHRAE [13], the general equation of heat balance for the room temperature is

$$\dot{Q}_c + \dot{Q}_h = M\frac{dT_i}{dt} \tag{1}$$

where M is the thermal inertia of the room, T_i is the average room temperature, and t is time. $\dot{Q}_c$ is the cooling power provided by the cooling cycle and $\dot{Q}_h$ is the room heat gain. In general, the heat gain may consist of different components as follows:

(1) direct heat gain: from electric equipment, light bulbs, human metabolic loads, etc.
(2) ambient heat gain: from convective and conductive heat transfer across walls
(3) ventilation heat gain: from infiltration/exfiltration of room air
(4) solar heat gain: from solar radiation on walls

The summation of the above heat gains equals the overall heat gain of the room, i.e., $\dot{Q}_h$. The instantaneous cooling power $\dot{Q}_c$

Table 1 Summary of recent RC models in HVAC-R applications. The digits before "R" and "C" means the number of resistances and capacitances used for the model, respectively. Parameter estimation method refers to the method of acquiring the resistance and capacitance values.

Authors	Envelope model	Room model	Parameters estimation method
Ogunsola et al. [19]	3R2C	2R2C[a]	Measurements (envelope) and genetic algorithm (room)
Maasoumy et al. [30]	4R1C	1C	Parameter adaptive building
Platt et al. [31]	1R	1C	Genetic algorithm
Bueno et al. [17]	3R2C	1C	Measurements
Oldewurtel et al. [29]	2R2C	1C	Stochastic MPC
Deng et al. [25]	3R2C	1C	Measurements
Mezrhab and Bouzidi [27]	2R2C	2R1C[a]	Measurements
Haldi and Robinson [26]	4R1C	1R1C[a]	Measurements
Zhu et al. [28]	3R2C[b]	1R1C[a]	Measurements
Wang and Xu [10]	3R2C	2R2C[a]	Genetic algorithm

[a]Resistance for room models is used to account for ventilation load, convection, or radiation from external sources.
[b]A 4R2C model is added to the wall in series to account for the layer of PCM.

depends on various characteristics of the cooling cycle as well as the room.

Assuming the ambient heat gain as the only available mechanism, the total heat gain is thus the summation of heat transfer across all walls

$$\dot{Q}_{\mathrm{h}} = \sum_{\text{walls}} \dot{Q}_{\mathrm{w}} \tag{2}$$

where $\dot{Q}_{\mathrm{w}}$ is the heat transfer rate across each wall. Applying the HBM, the heat flow across a wall crosses an outside convective resistance, a wall conductive RC, and an inside convective resistance. Thus, the following relationships hold:

$$\dot{Q}_{\mathrm{w}} = h_{\mathrm{o}} A(T_{\mathrm{o}} - T_{\mathrm{wo}}) = \frac{k}{b} A(T_{\mathrm{wo}} - T_{\mathrm{wi}}) + \rho_{\mathrm{w}} b A c_{\mathrm{w}} \frac{d(T_{\mathrm{wo}} - T_{\mathrm{wi}})}{dt} = h_{\mathrm{i}} A(T_{\mathrm{wi}} - T_{\mathrm{i}}) \tag{3}$$

where h_{o} and h_{i} are outside and inside convective coefficients, respectively. A is wall surface area, k is wall thermal conductivity, b is wall thickness, ρ_{w} is wall density, and c_{w} is wall specific heat. T_{o} and T_{i} are the outside and inside temperatures, respectively. T_{wo} and T_{wi} are the temperatures on the outside and inside wall surfaces, respectively.

Thermal convective and conductive resistances are defined as $R_h = 1/hA$ and $R_k = b/kA$, respectively. Thermal inertia is defined as $M = mc$, where m is mass and c is specific heat. Specifically, thermal inertia is defined as $M_{\mathrm{w}} = \rho_{\mathrm{w}} b A c_{\mathrm{w}}$ for walls. Using these conventions, Eq. (3) is rewritten as

$$\dot{Q}_{\mathrm{w}} = \frac{T_{\mathrm{o}} - T_{\mathrm{wo}}}{R_{h\mathrm{o}}} = \frac{T_{\mathrm{wo}} - T_{\mathrm{wi}}}{R_k} + M_{\mathrm{w}} \frac{d(T_{\mathrm{wo}} - T_{\mathrm{wi}})}{dt} = \frac{T_{\mathrm{wi}} - T_{\mathrm{i}}}{R_{h\mathrm{i}}} \tag{4}$$

Equation (1) should be solved for the heat balance analysis of the room using Eqs. (2) and (4) for calculation of heat gains. The solution process is facilitated by considering the identical electric circuit and simulating it.

2.2 RC Model. Simulating a thermal system using an RC model consists of finding its equivalent electric circuit. Once the circuit is set up, the values of its components are found according to their corresponding thermal quantities. Temperature T in a thermal system is equivalent to voltage V in an electric system while the equivalent of heat flow rate Q is current I. Thermal resistances R_h and R_k are equivalent to electric resistance R, and thermal inertia M is identical to electric capacitance C. By appropriate selection of parameters, the governing equations of both thermal and electric systems are the same. Thus, the solution to the electric circuit is the same as the solution to its identical thermal problem. Using the following identities

$$Q = \frac{\Delta T}{R_h \text{or} R_k} \quad \equiv \quad I = \frac{\Delta V}{R} \tag{5}$$

$$Q = M_{\mathrm{w}} \frac{dT}{dt} \quad \equiv \quad I = C_{\mathrm{w}} \frac{dV}{dt} \tag{6}$$

we obtain the following equation:

$$I = \frac{V_{\mathrm{o}} - V_{\mathrm{wo}}}{R_{\mathrm{o}}} = \frac{V_{\mathrm{wo}} - V_{\mathrm{wi}}}{R_{\mathrm{w}}} + C_{\mathrm{w}} \frac{d(V_{\mathrm{wo}} - V_{\mathrm{wi}})}{dt} = \frac{V_{\mathrm{wi}} - V_{\mathrm{i}}}{R_{\mathrm{i}}} \tag{7}$$

Equation (7) is the governing equation of the circuit shown in Fig. 1. Thus, the equivalent electric circuit of a wall in a thermal system is as shown in Fig. 1.

The subcircuit shown in Fig. 1 is a 3R1C representation of a wall. In this work, a 1C model is considered for the room air. Hence, the aggregate of the room air and the products stored in it is assumed to have a bulk thermal inertia represented by an identical capacitance.

As demonstrated here, the methodology associated to RC modeling is general and can be applied to a wide range of HVAC-R applications. Once the RC network of a specific application is generated, it can be easily used for design, retrofit analysis, and parametric study of the thermal system with considerable ease and accuracy. In Sec. 3, a case study is performed on a refrigeration application and the RC modeling results are compared with experimental measurements.

3 Case Study

The proposed RC modeling technique is demonstrated using a refrigeration application. Temperature measurements in the freezer room of a restaurant in Surrey, British Columbia, Canada are studied during more than 5 months of its normal operation. Figure 2 shows an inside view of the freezer as well as its schematic with inner room dimensions. Information about the room dimensions, insulation properties, and stored products are carefully gathered and used in the RC model.

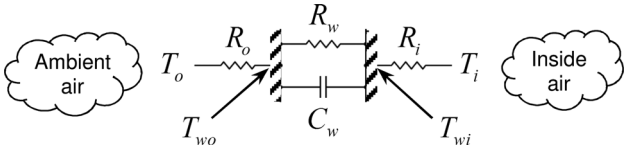

Fig. 1 Analogous 3R1C electric circuit of a wall heat balance equation in RC modeling

The freezer temperature is measured over time using Rotronic LOG-HC2-RC-US wireless data loggers installed on arbitrary shelves. The measurement accuracy is $\pm 0.1\,^{\circ}\mathrm{C}$ within the range of $-40\,^{\circ}\mathrm{C}$ to $+85\,^{\circ}\mathrm{C}$. It is observed that a nonuniformity of less than $\pm 2\,^{\circ}\mathrm{C}$ exists throughout the room. Thus, the measured values of one of the loggers are assumed as the room bulk temperature.

Table 2 shows the dimensional, material, and thermal properties of the freezer room. Convective heat transfer coefficients are estimated using correlations from ASHRAE [13] for turbulent natural convection on vertical and horizontal flat plates. The ASHRAE coefficient of air natural convection over a vertical wall is calculated from

$$h = 1.33\left(\frac{T_a - T_w}{H}\right)^{1/4} \tag{8}$$

where H is the wall height and T_a is the air temperature. The coefficient of air natural convection over a horizontal surface is calculated from

$$h = K\left(\frac{g\beta\rho_a^2 k_a^3 c_a P}{\mu_a A}(T_a - T_w)\right)^{1/4} \tag{9}$$

where g is the gravitational constant, β is the volumetric coefficient of thermal expansion, ρ_a is the air density, k_a is the air thermal conductivity, c_a is the air specific heat, P is the wall perimeter, and μ_a is the air dynamic viscosity. $K = 0.54$ for a cold surface facing down and $K = 0.27$ for a cold surface facing up.

Figure 3 shows the measured freezer temperature during 2000 min of its operation. Three distinct patterns of temperature variation are visible in Fig. 3.

Temperature Swings. Temperature swings, i.e., temperature oscillations, occur mainly due to the starts and stops of the refrigeration unit. In Fig. 3, the arrows show durations of temperature swinging. The period of these oscillations in the current application is approximately 20 min. The studied freezer, similar to most existing refrigeration systems, is controlled based on low and high temperature set points. The system produces cooling until the room temperature reaches the low temperature set point. Once the low set point is reached, the thermostat shuts the refrigeration unit down. At this point, the pulling down of the room temperature stops and the temperature begins to increase as a result of heat gains. The room temperature then increases until it reaches the high temperature set point. Once the high set point is reached, the thermostat triggers the refrigeration unit to turn back on.

The low and high temperature set points for the studied refrigeration system are $-15.3\,^{\circ}\mathrm{C}$ and $-11.4\,^{\circ}\mathrm{C}$, respectively. Of course, these set point values depend on the sensor location. However, although the resulting set points observed at the sensor location can vary from one point to another, the modeling approach is valid as long as those sensor-specific set points are used in the RC circuit.

Temperature Spikes. Temperature spikes, i.e., rapid temperature increases, are noticeable in some parts of Fig. 3 denoted by circles. These spikes are due to automatic defrost events. Defrosting is a process that melts the frost away from evaporator coils and is unavoidable for most systems. The defrost system can work either by heating the pipes or turning off the refrigeration system [32]. The defrost system in the studied freezer operates every 6 hr. The defrost events, even though a necessity, impose an amount of heat load on the freezer room, as perceived by the sharp temperature increases in Fig. 3.

Door Openings. Door openings, i.e., periods of time when the freezer door is opened for a few times, are denoted by a bracket in Fig. 3. During these periods of time, irregular variations in the freezer temperature are observed. Since the temperature is mostly above the set points, the refrigeration system is constantly working during these periods. The loading and unloading of goods in the freezer room are the main reasons for the occurrence of such door opening events.

The majority of the service time for many freezers including the one studied here corresponds to the temperature swings observed in Fig. 3. Door openings and defrosts are generally rare compared to closed door operation of the freezer near its set points. Nevertheless, the door openings can be unpredicted and irregular depending on the usage pattern of the freezer in the specific application. A long-term study of the room temperature can lead to an estimation of the duty cycle and the cooling load imposed by door openings.

In this study, the focus is on the temperature swings of the freezer and a model is developed for cooling load simulation

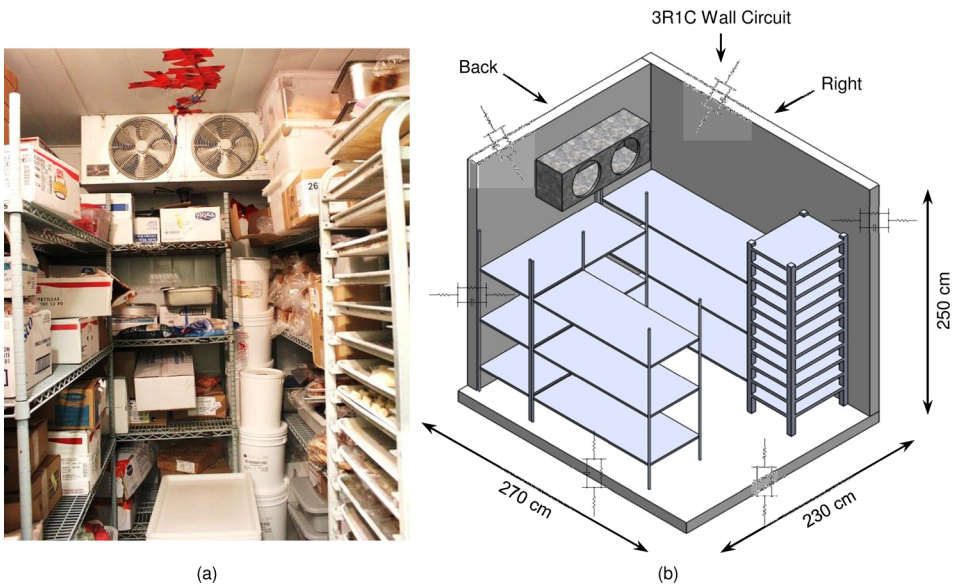

Fig. 2 (*a*) Walk-in freezer room. (*b*) Freezer schematic with inner room dimensions. The front wall, left wall, and roof are omitted for clarity.

Table 2 Dimensional, material, and thermal properties of the freezer room. Refer to Fig. 2 for wall locations.

Quantity	Units	Wall no. 1	2	3	4	5	6
Location	—	Left	Back	Right	Front	Roof	Floor
Area, A	(m^2)	6.7	5.7	6.7	5.7	6.2	6.2
Outside convective coefficient, h_o	($W/m^2\,°C$)	2.8	2.8	2.8	2.8	0.6	3.1
Inside convective coefficient, h_i	($W/m^2\,°C$)	2.8	2.8	2.8	2.8	0.6	3.1
Insulation thickness	(mm)			30			
Total wall thickness, b	(mm)			110			
Insulation material	—			Polyurethane foam			
Wall thermal conductivity, k	(W/m °C)			0.05			
Wall density, ρ_w	(Kg/m^3)			22			
Wall specific heat, c_w	(kJ/kg °C)			2.6			

during such periods. The freezer studied in this work is indoors, and there is negligible solar radiation on it. There is no significant source of direct heat in the room and human metabolic load is only imposed to the system during door openings. During the temperature swings (pointed by arrows in Fig. 3), the freezer door is closed and the amount of infiltration/exfiltration of air is negligible. Hence, the only available heat source in the studied time periods is the ambient heat gain which is in compliance to the assumption made in the model development. Other heat gain mechanisms can be later added to the model in order to include the door opening and defrost loads.

An RC model of the refrigerator is prepared as demonstrated in Fig. 4. Figure 4 also shows the value of the circuit components according to their definitions and the properties presented in Table 2. In the main body of the circuit, six parallel wall blocks (Fig. 1) are considered. Each of the six wall branches in the circuit represents one of the freezer walls. In series to the six-layer block, a capacitor C is inserted that represents the overall thermal inertia M of the air and products in the freezer.

The room air and its products have an estimated overall thermal inertia of 100 kJ/ °C. This value is calculated by measuring the mass of every product in the freezer. By multiplying the product's mass in its estimated specific heat and summing for all the freezer contents, the overall value is calculated. The thermal inertia of the room envelope is not included in this value, since it is considered in the corresponding wall capacitors. Assuming a combined mass of 100 kg for the miscellaneous objects including the evaporator coils and shelves, and using an average specific heat of 0.6 kJ/kg °C for the metallic components, the total miscellaneous thermal inertia is calculated as 60 kJ/ °C. Table 3 shows a list of the food products left in the room during the experiments of this specific study. Therefore, a bulk capacitance of $C = 100\,\text{kJ/}°\text{C}$ is considered for the room.

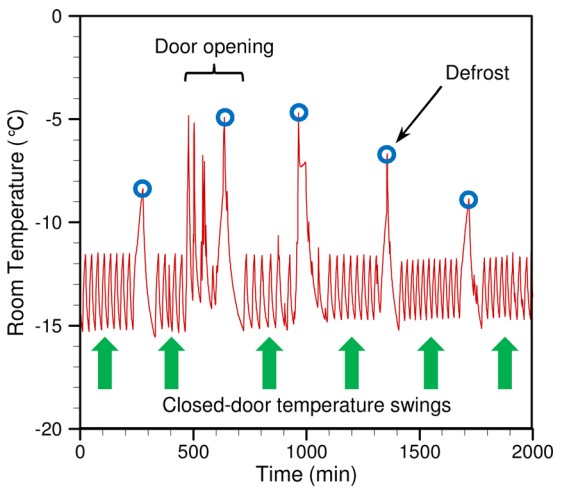

Fig. 3 Measured freezer temperature during 2000 min of its operation. Arrows show temperature swings, circles show temperature spikes, and the bracket shows door opening events.

The voltage difference between the two sides of the capacitor C represents the difference between the freezer temperature and the outside temperature. According to the measurements, outside temperature has been kept at a value of 25±1 °C during the period under consideration. This value is added to the aforementioned temperature difference in the circuit (Fig. 4). According to the manufacturer information and analysis of the refrigeration unit, it is estimated that the refrigeration cycle provides an average amount of $\dot{Q}_c = 950\,\text{W}$ cooling capacity to the room when the temperature is near the set point values. Temperature variations of Fig. 3 are studied to find the approximate low and high set points for the freezer. The low set point is observed to be −15.3 °C, while the high set point is approximately found equal to −11.4 °C.

Between the six parallel RC blocks, a current source is inserted which represents the cooling load provided by the refrigeration system. Since the cooling load does not cross any wall and is directly transferred to the room, this heat source is implemented parallel to the walls. The current direction is shown toward the room. Therefore, a negative cooling load is considered as the input value to this source.

In this study, the ventilation load due to door openings is not considered. In a future study, further information on the occurrence of door openings and their duration can be incorporated in the model. Those data can be inserted in appropriate correlations to find the overall ventilation heat gain imposed to the system in each door opening occurrence. Furthermore, the radiation loads can also be incorporated in the model as another mode of heat gain into the room. In that case, the ventilation and radiation heat gains can be simply added to the "current source" included in the middle of the RC model of Fig. 4.

The operational logic of the cooling cycle is implemented in the RC model shown on the top part of Fig. 4. Starting from when the room is warm, the refrigeration system works until the low set point temperature is reached. Afterward, the cooling cycle shuts down and the room gains heat through the walls. As a result, the room temperature increases until it reaches the high set point. At the high set point, the cycle restarts working to pull the room temperature down to the low set point again. This process continues and creates a swinging regime in the temperature variation pattern. Evidently, since the heat transfer is proportional to the temperature differences across the walls, the temperature decrease and increase processes are exponential.

MATLAB Simulink [33] is used to implement and solve the RC model. The transient solution is solved using the software, and the results are compared to measured freezer temperatures. The results are discussed in Section 4.

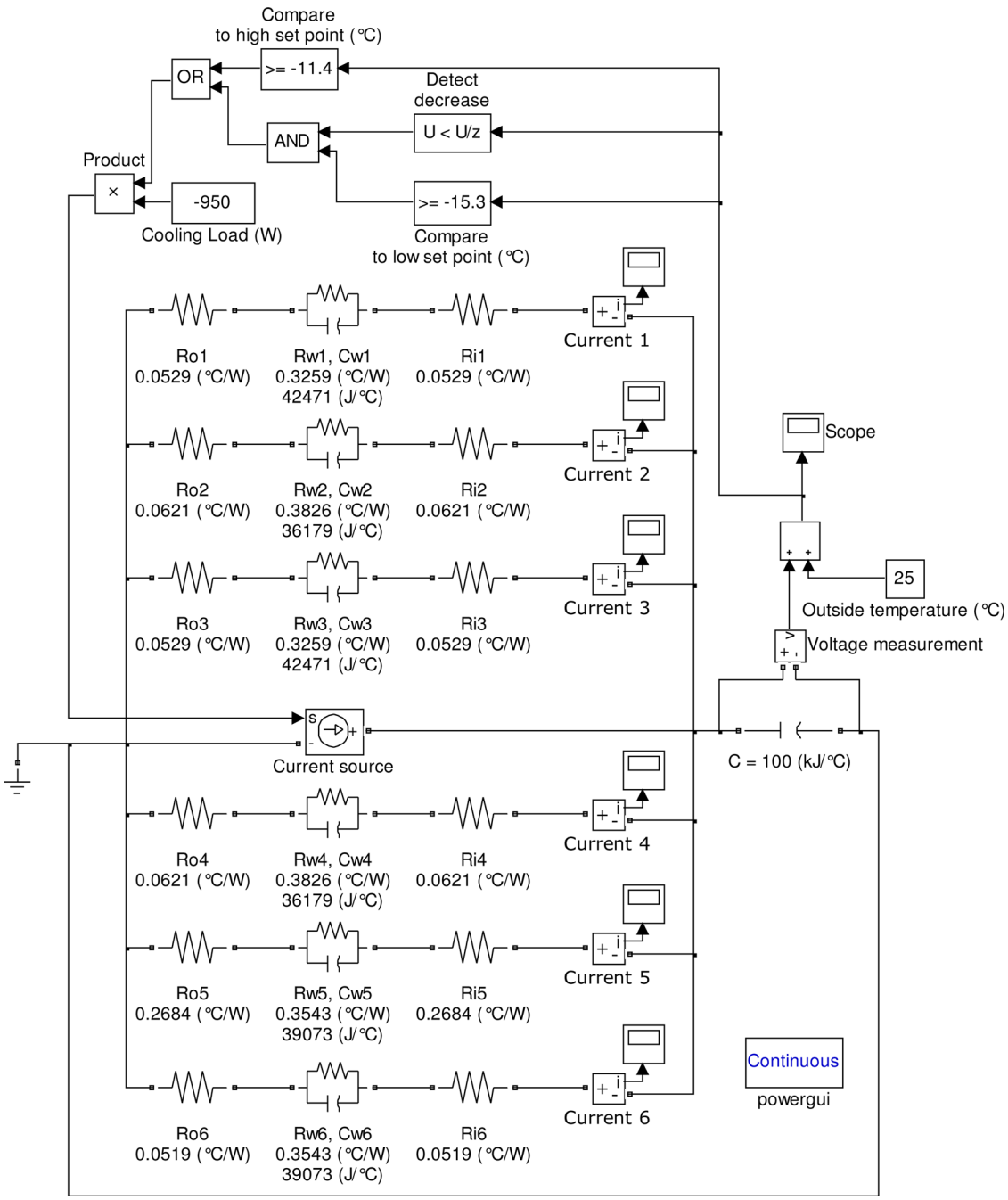

Fig. 4 RC model of the refrigeration system. 3R1C and 1C models are used for the walls and the room, respectively.

4 Validation and Results

The transient solution of the RC model of Fig. 4 is compared to the temperature measurements inside the freezer room. Figure 5 shows a comparison between the present model and the measured temperature during 200 min of the freezer operation. Refer to Fig. 3 for a wider range of temperature measurements including defrost and door opening events. During the studied period of Fig. 5, the freezer door is not open and the temperature is already within the range of the set points. This condition covers most of the service period of many refrigeration rooms.

Temperature measurement uncertainty for the experimental results shown in Fig. 5 is less than 0.1 °C. Maximum discrepancy between the measurements and the RC model is less than 1 °C. The RC model shows good agreement with the freezer temperature measurements.

Degradation of thermal insulation materials is a serious issue in long-term applications. Polyurethane insulators are prone to degradation which decreases their thermal resistivity over time. The present model is used to study the effect of thermal degradation

Table 3 List of masses and specific heats for the stored products and miscellaneous components in the freezer room

Product	Mass (kg)	Thermal inertia (kJ/°C)
Peas	12	11.04
Sweet potato fries	7.5	11.93
Corn	12	17.04
Miscellaneous parts	100	60.00
Total	137.46	100.01

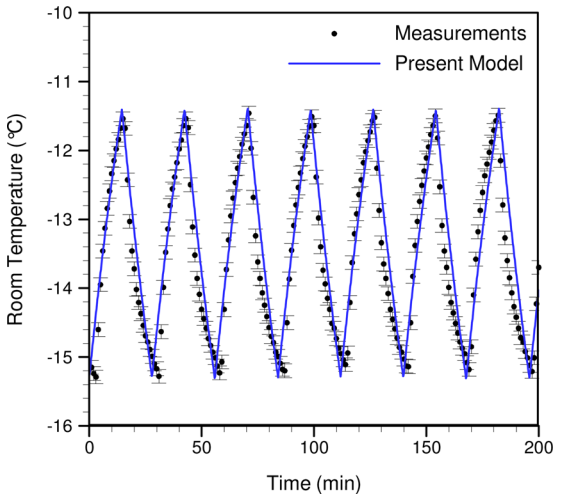

Fig. 5 RC model results compared to measured freezer temperature during 200 min of its operation. Maximum discrepancy of less than between the measurements and the present model is observed.

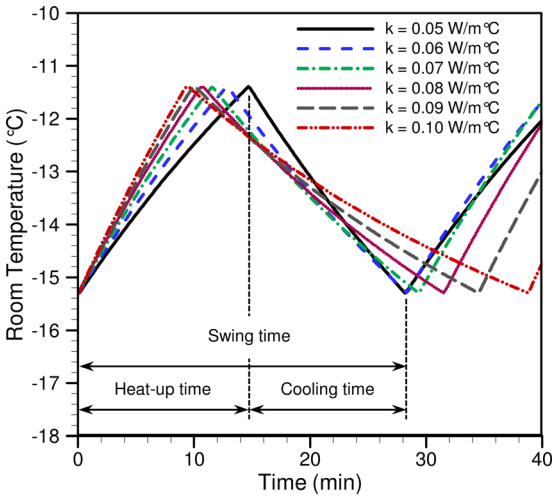

Fig. 6 Effect of wall thermal conductivity *k* on temperature swings in the freezer room

on the overall energy consumption of the freezer system. Figure 6 shows the freezer temperature during 40 min of its operation. The walls thermal conductivity is varied from $k = 0.05\,\mathrm{W/m\,^{\circ}C}$ to $k = 0.10\,\mathrm{W/m\,^{\circ}C}$. As demonstrated in Fig. 6, an instant of temperature swing can be divided into a heat-up portion when the temperature increases due to heat gains and a cooling portion when the temperature decreases due to the operation of the cooling system. During the heat-up period, the cooling cycle is off and consumes no energy. On the other hand, during the cooling period, the cooling cycle is on and provides $\dot{Q}_c = 950\,\mathrm{W}$ of cooling load to the freezer. The ratio of the cooling time to the total swing time is defined as

$$r = \frac{\text{cooling time}}{\text{swing time}} \tag{10}$$

where r is the cooling time ratio. The swing time is defined as the total time between two consecutive low set points in the temperature graph, as shown in Fig. 6. The cooling time ratio r represents the portion of time that the refrigeration cycle is on and produces cooling effect. By multiplying the cooling time ratio by the instantaneous cooling load, the net cooling effect $\dot{Q}_{net}$ is calculated as

$$\dot{Q}_{net} = r\dot{Q}_c \tag{11}$$

The net cooling effect $\dot{Q}_{net}$ is the average cooling power provided by the refrigeration cycle during temperature swings. Since the overall power consumption of the cooling cycle is directly proportional to the provided net cooling effect, higher values of $\dot{Q}_{net}$ result in higher power consumption by the entire system.

Table 4 shows the cooling time ratio r for different wall conductivities k and their corresponding net cooling effects $\dot{Q}_{net}$. The power consumption increase in Table 4 shows the percentage of increase in the refrigeration power consumption due to insulation degradation compared to the current condition of the freezer, i.e., walls with $k = 0.05\,\mathrm{W/m\,^{\circ}C}$. As shown in Table 4, a reduction of 20% in the walls thermal resistivity from the current value can increase the energy consumption rate by 14.87%. Once the walls thermal resistivity reduces to half, a considerable power consumption increase of 57.05% is expected. There is thus a tremendous opportunity in replacing the wall insulation regularly and the insulation cost can be paid off by the decrease in wasted energy during the operation of the freezer. The RC model is beneficial for estimating the power loss which can be used as a criterion for the timing of insulation renewals.

Figure 7 shows the effect of different set point values on the temperature swing pattern of the freezer room during 40 min of its operation. When the set points are narrow, i.e., the values of the high and low set points are close to each other, the frequency of the oscillations is high and the swing time is low. As shown is Fig. 7, three different set point pairs are studied. All set point pairs are mirrored around the same average temperature, i.e., $T_{average} = 13.35\,^{\circ}\mathrm{C}$. The swing time is again defined as the total time between two consecutive low set points in the temperature graph. Maximum temperature deviation for each set point pair is the absolute difference between the average temperature and the high or low set point.

Table 5 demonstrates a comparison of the swing time for different set points of the cooling cycle. The maximum temperature deviation is also shown in Table 5. Generally, it is required to keep the products temperature constant at the design level and deviations from the average value are not desirable. To achieve less temperature deviations, narrower set point pairs can be implemented in the freezer thermostats and the products will experience less temperature variation as a result. A drawback of using narrow set point pairs is that the swing time decreases as well. This results in increased number of compressor starts/stops per hour. Compressor manufacturers normally recommend limited numbers of starts/stops per hour to assure proper operation during the designed lifetime of the compressor. Furthermore, compressors draw a high amount of energy at every startup. This increased power draw also increases the overall power consumption of the refrigeration system. Thus, it is required to keep the number of compressor starts/stops within a certain limit.

Table 5 shows that by changing the set points, the maximum temperature deviation can be reduced to $0.3\,^{\circ}\mathrm{C}$, but the swing time would decrease to 2.59 min and an average of 24 compressor starts/stops per hour would be required. Nevertheless, the system can be allowed to have 14 compressor starts/stops per hour to

Table 4 Comparison of the required net cooling effect for different freezer wall thermal conductivity values

Wall thermal conductivity k(W/m °C)	Cooling time ratio (r)	Net cooling effect $\dot{Q}_{net}$ (W)	Power consumption increase (%)
0.05	0.48	457.17	0.00
0.06	0.55	525.13	14.87
0.07	0.61	576.42	26.08
0.08	0.66	628.52	37.48
0.09	0.71	674.83	47.61
0.10	0.76	717.97	57.05

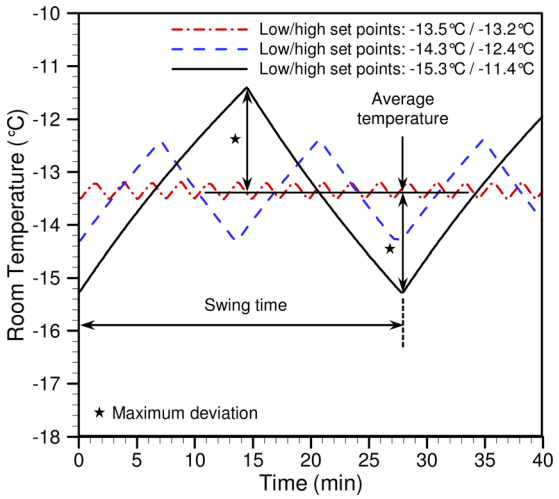

Fig. 7 Effect of set points on temperature swings in the freezer room

Table 5 Comparison of swing time and temperature deviation for different set points

Low/high temperature set points (°C)	Swing time (min)	Starts/stops per hour (1/hr)	Maximum temperature deviation (°C)
−13.5/−13.2	2.59	23.17	0.3
−14.3/−12.4	13.5	4.44	0.95
−15.3/−11.4	27.86	2.15	1.95

provide a maximum temperature deviation of less than 1 °C. The RC model can be an advantageous tool for predicting the temperature variation pattern for different set point pairs. Eventually this tool helps estimate the trade-off between the maximum temperature deviation and the number of compressor starts/stops per hour.

In summary, the proposed RC model can help HVAC-R designers gain an understanding of the real-time effect of several parameters on their design. As an example, the effect of insulation degradation on the net power consumption of the freezer is studied. It is also shown that HVAC-R designers can use the RC modeling technique to select the freezer temperature set points with a proper approximation of the required number of compressor starts/stops per hour.

5 Conclusions

In this study, an RC model was developed that utilizes a representative network of electric resistors and capacitors to accurately simulate the thermal behavior of HVAC-R systems in real-time. As an example, a freezer room of a restaurant during its operation was used. Corresponding thermal parameters were introduced and combined to design the analogous RC circuit. The model was validated by actual freezer temperature measurements. The present RC model has the following features:

- real-time simulation capability
- proactive control
- unsophisticated mathematical algorithms
- one RC circuit for an entire system
- validated with experimental data
- usability for retrofit analysis

The proposed RC model proved to be an effective tool for facilitating thermal modeling as well as acquiring accurate predictions of the system behavior in real-time. The room heat gain was estimated using the model. Parametric study was performed on the effect of insulation degradation on the net power consumption by the refrigeration cycle. It was shown that 20% degradation of the insulation can result in around 15% of increase in the net power consumption by the cooling cycle. The effect of set points on the number of compressor starts/stops was also studied, and it was shown that narrow set points can result in a steady temperature pattern in exchange for a high number of compressor starts/stops per hour. Using the RC modeling methodology, engineering calculations of cooling load in HVAC-R applications can be performed with outstanding simplicity and accuracy.

Acknowledgment

This work was supported by Automotive Partnership Canada (APC), Grant No. NSERC APCPJ/429698-11. The authors would like to thank the support of the Central City Brew Pub, 13450 102nd Avenue, Surrey, BC.

Nomenclature

A = wall surface area (m^2)
b = wall thickness (mm)
c = specific heat (J/kg °C)
C = capacitance (F)
h = convective coefficient (W/m^2 °C)
H = wall height (m)
I = current (A)
k = thermal conductivity (W/m °C)
K = correlation constant
m = mass (kg)
M = thermal inertia (J/°C)
$\dot{Q}$ = heat flow (W)
$\dot{Q}_{net}$ = net cooling effect (W)
r = cooling time ratio
R = electric resistance (Ω)
R_h = convective resistance (°C/W)
R_k = conductive resistance (°C/W)
t = time (s)
T = temperature (°C)
V = voltage (v)

Greek Symbols

β = volumetric coefficient of thermal expansion (1/K)
μ = viscosity (Ns/m^2)
ρ = density (kg/m^3)

Subscripts

a = air
c = cooling
h = heat gain
i = inside
o = outside
w = wall

References

[1] Pérez-Lombard, L., Ortiz, J., and Pout, C., 2008, "A Review on Buildings Energy Consumption Information," Energy Build., **40**(3), pp. 394–398.
[2] Chua, K. J., Chou, S. K., Yang, W. M., and Yan, J., 2013, "Achieving Better Energy-Efficient Air Conditioning–A Review of Technologies and Strategies," Appl. Energy, **104**, pp. 87–104.
[3] Hovgaard, T., Larsen, L., Skovrup, M., and Jørgensen, J., 2011, "Power Consumption in Refrigeration Systems-Modeling for Optimization," 2011 4th International Symposium on Advanced Control of Industrial Processes, Hangzhou, China, May 23–26, pp. 234–239.
[4] Farrington, R., and Rugh, J., 2000, "Impact of Vehicle Air-Conditioning on Fuel Economy, Tailpipe Emissions, and Electric Vehicle Range," Earth Technologies Forum, pp. 1–6.
[5] Lambert, M. A., and Jones, B. J., 2006, "Automotive Adsorption Air Conditioner Powered by Exhaust Heat—Part 1: Conceptual and Embodiment Design," Proc. Inst. Mech. Eng., Part D, **220**(7), pp. 959–972.
[6] Farrington, R., Cuddy, M., Keyser, M., and Rugh, J., 1999, "Opportunities to Reduce Air-Conditioning Loads Through Lower Cabin Soak Temperatures," Proceedings of the 16th Electric Vehicle Symposium, pp. 1–9.

[7] Ansari, F., and Mokhtar, A., 2005, "A Simple Approach for Building Cooling Load Estimation," Am. J. Environ. Sci., **1**(3), pp. 209–212.
[8] Kashiwagi, N., and Tobi, T., 1993, "Heating and Cooling Load Prediction Using a Neural Network System," 1993 International Conference on Neural Networks (IJCNN-93), Nagoya, Japan, Oct. 25–29, Vol. 1, pp. 939–942.
[9] Ben-Nakhi, A. E., and Mahmoud, M. a., 2004, "Cooling Load Prediction for Buildings Using General Regression Neural Networks," Energy Convers. Manage., **45**(13–14), pp. 2127–2141.
[10] Wang, S., and Xu, X., 2006, "Parameter Estimation of Internal Thermal Mass of Building Dynamic Models Using Genetic Algorithm," Energy Convers. Manag., **47**(13–14), pp. 1927–1941.
[11] Wang, S., and Xu, X., 2006, "Simplified Building Model for Transient Thermal Performance Estimation Using GA-Based Parameter Identification," Int. J. Therm. Sci., **45**(4), pp. 419–432.
[12] Sousa, J. M., Babuška, R., and Verbruggen, H. B., 1997, "Fuzzy Predictive Control Applied to an Air-Conditioning System," Control Eng. Pract., **5**(10), pp. 1395–1406.
[13] ASHRAE, 2009, *Handbook of Fundamentals*, American Society of Heating, Refrigerating and Air-Conditioning, Atlanta, GA.
[14] Pedersen, C. O., Fisher, D. E., and Liesen, R. J., 1997, "Development of a Heat Balance Procedure for Calculating Cooling Loads," ASHRAE Trans., **103**, pp. 459–468.
[15] Barnaby, C. S., Spitler, J. D., and Xiao, D., 2005, "The Residential Heat Balance Method for Heating and Cooling Load Calculations," ASHRAE Trans., **111**(1), pp. 308–319.
[16] Fayazbakhsh, M. A., and Bahrami, M., 2013, "Comprehensive Modeling of Vehicle Air Conditioning Loads Using Heat Balance Method," SAE International Paper No. 2013-01-1507.
[17] Bueno, B., Norford, L., Pigeon, G., and Britter, R., 2012, "A Resistance-Capacitance Network Model for the Analysis of the Interactions Between the Energy Performance of Buildings and the Urban Climate," Build. Environ., **54**, pp. 116–125.
[18] Yener, Y., and Kakaç, S., 2008, *Heat Conduction*, Taylor & Francis Group, New York.
[19] Ogunsola, O. T., Song, L., and Wang, G., 2014, "Development and Validation of a Time-Series Model for Real-Time Thermal Load Estimation," Energy Build., **76**, pp. 440–449.
[20] Zhao, R., Gosselin, L., Fafard, M., and Ziegler, D. P., 2013, "Heat Transfer in Upper Part of Electrolytic Cells: Thermal Circuit and Sensitivity Analysis," Appl. Therm. Eng., **54**(1), pp. 212–225.
[21] El-Nasr, A. A., and El-Haggar, S. M., 1996, "Effective Thermal Conductivity of Heat Pipes," Heat Mass Transfer, **32**(1–2), pp. 97–101.
[22] Moghaddam, S., Rada, M., Shooshtari, A., Ohadi, M., and Joshi, Y., 2003, "Evaluation of Analytical Models for Thermal Analysis and Design of Electronic Packages," Microelectron. J., **34**(3), pp. 223–230.
[23] Gholami, A., Ahmadi, M., and Bahrami, M., 2014, "A New Analytical Approach for Dynamic Modeling of Passive Multicomponent Cooling Systems," ASME J. Electron. Packag., **136**(3), p. 031010.
[24] Shi, W., Wang, B., and Li, X., 2005, "A Measurement Method of Ice Layer Thickness Based on Resistance-Capacitance Circuit for Closed Loop External Melt Ice Storage Tank," Appl. Therm. Eng., **25**(11–12), pp. 1697–1707.
[25] Deng, K., Barooah, P., Mehta, P. G., and Meyn, S. P., 2010, "Building Thermal Model Reduction Via Aggregation of States," American Control Conference, pp. 5118–5123.
[26] Haldi, F., and Robinson, D., 2010, "The Impact of Occupants' Behaviour on Urban Energy Demand," BauSim 2010, pp. 343–348.
[27] Mezrhab, A., and Bouzidi, M., 2006, "Computation of Thermal Comfort Inside a Passenger Car Compartment," Appl. Therm. Eng., **26**(14–15), pp. 1697–1704.
[28] Zhu, N., Wang, S., Ma, Z., and Sun, Y., 2011, "Energy Performance and Optimal Control of Air-Conditioned Buildings With Envelopes Enhanced by Phase Change Materials," Energy Convers. Manag., **52**(10), pp. 3197–3205.
[29] Oldewurtel, F., Parisio, A., Jones, C. N., Gyalistras, D., Gwerder, M., Stauch, V., Lehmann, B., and Morari, M., 2012, "Use of Model Predictive Control and Weather Forecasts for Energy Efficient Building Climate Control," Energy Build., **45**, pp. 15–27.
[30] Maasoumy, M., Razmara, M., Shahbakhti, M., and Vincentelli, A. S., 2014, "Handling Model Uncertainty in Model Predictive Control for Energy Efficient Buildings," Energy Build., **77**, pp. 377–392.
[31] Platt, G., Li, J., Li, R., Poulton, G., James, G., and Wall, J., 2010, "Adaptive HVAC Zone Modeling for Sustainable Buildings," Energy Build., **42**(4), pp. 412–421.
[32] Allard, J., and Heinzen, R., 1988, "Adaptive Defrost," IEEE Trans. Ind. Appl., **24**(1), pp. 39–42.
[33] The MathWorks, Inc., 2011, *MATLAB Version R2011b*, The MathWorks, Inc., Natick, MA.